Am J Transl Res 2024;16(4):1306-1321
www.ajtr.org /ISSN:1943-8141/AJTR0154766

Original Article

Unveiling the unexplored novel signatures for osteoporosis via a detailed bioinformatics and molecular experiments based approach

Huan Zhou[1], Yousaf Gul[2], Yasir Hameed[3], Majid Alhomrani[4,5], Saleh A Alghamdi[4], Abdulraheem Ali Almalki[4], Meshari A Alsuwat[4], Naif ALSuhaymi[6], Rida Naz[7], Guang Chen[8]

[1]Department of Medical Oncology, The Second Hospital of Dalian Medical University, Dalian, Liaoning, China; [2]Gomal Medical College, District Headquarter Teaching Hospital Dera Ismail Khan, KPK, Pakistan; [3]Department of Biotechnology, Institute of Biochemistry Biotechnology, and Bioinformatics, The Islamia University of Bahawalpur, Pakistan; [4]Department of Clinical Laboratory Sciences, College of Applied Medical Sciences, Taif University, Taif, Saudi Arabia; [5]Research Centre for Health Sciences, Taif University, Taif 21944, Saudi Arabia; [6]Department of Emergency Medical Services, Faculty of Health Science-AlQunfudah, Umm Al-Qura University, Makkah 21955, Saudi Arabia; [7]Regional Blood Centre, KPK Health Program, Dera Ismail Khan 29050, Pakistan; [8]Department of Orthopedic Surgery, The Second Hospital of Dalian Medical University, Dalian, Liaoning, China

Received December 4, 2023; Accepted March 27, 2024; Epub April 15, 2024; Published April 30, 2024

Abstract: Background: Osteoporosis (OP) stands as a prevalent bone ailment affecting the elderly, globally. The identification of reliable diagnostic markers crucially aids OP clinical management. Methods: Utilizing the GEO database (GSE35959), we acquired expression profiles for OP and normal samples. Differential expression genes (DEGs) and hub genes were pinpointed through STRING, GEO2R, and Cytoscape. The competing endogenous RNA (ceRNA) network was constructed using miRTarBase, miRDB, and MiRcode databases. Gene Ontology (GO) and KEGG pathway enrichment analyses were performed via DAVID. Validation involved clinical OP samples from the Pakistani population, with Real-Time Quantitative Polymerase Chain Reaction (RT-qPCR) assessing hub gene expression. Results: A total of 2124 differentially expressed genes (DEGs) were identified between OP and normal samples in GSE35959. The selected hub genes among these DEGs were Splicing Factor 3a Subunit 1 (SF3A1), Ataxin 2 Like (ATXN2L), Heat Shock Protein 90 Beta Family Member 1 (HSP90B1), Cluster of Differentiation 74 (CD74), DExH-Box Helicase 29 (DHX29), ALG5 Dolichyl-Phosphate Beta-Glucosyltransferase (ALG5), NudC Domain Containing 2 (NUDCD2), and Ras-related protein Rab-2A (RAB2A). Expression validation of these genes on the Pakistani OP patients revealed significant up-regulation of SF3A1, ATXN2L, and CD74 and significant ($P < 0.05$) down-regulation of HSP90B1, DHX29, ALG5, NUDCD2, and RAB2A in OP patients. Receiver operating characteristic (ROC) analysis demonstrated that these hub genes displayed considerable diagnostic accuracy for detecting OP. The ceRNA network analysis of the hub genes revealed some important hub genes' regulatory miRNAs and lncRNAs. Via KEGG analysis, hub genes were found to be enriched in N-Glycan biosynthesis, Thyroid hormone synthesis, IL-17 signaling pathway, Prostate cancer, AMPK signaling pathway, Spliceosome, Estrogen signaling pathway, and Fluid shear stress and atherosclerosis, etc., pathways. Conclusion: The identified eight hub genes in the present study could reliably distinguish OP patients from normal individuals, which may provide novel insight into the diagnostic research of OP.

Keywords: Osteoporosis (OP), diagnostic signatures, AMPK signaling pathway

Introduction

Osteoporosis (OP), which is mainly characterized by impaired bone microarchitecture and the loss of bone mass and strength, has emerged as a significant clinical issue in aging populations [1, 2]. The most commonly fractured site for OP is the spine, while other less common sites include the hip, forearm, and proximal humerus [3].

According to medical literature, there are a variety of contributing factors for the development and progression of this disease, including genetic abnormalities, gender, age, steroid production, lifestyle, and other environmental factors [4-6]. In addition to these factors, less intake of calcium, cigarette smoking, and excessive alcohol drinking are the secondary contributing factors to OP [7, 8]. In general, this disease is known as a "silent disease" due

https://doi.org/10.62347/TAYD3318

to its asymptomatic nature until a fracture happens.

Currently, OP treatment methods include the use of medicines, but this treatment method is not satisfactory because of its time-consuming nature and high cost, as well as due to the adverse side effects of the medicine. So far, different researchers around the world have tried to explore the underlying mechanisms of OP. For example, one study reported that the members of the Wnt signaling pathway, including Wnt3a, secreted frizzled-related protein 1, sclerostin, and low-density lipoprotein receptor-related protein 5, are related to the changes in bone mineral density (BMD) inside the bones [9]. Measurement of BMD (with heritability estimates of 0.5 to 0.9) is an important parameter to clinically define the occurrence of OP [10]. Therefore, BMD measurement is a vital clinical biomarker of OP. However, the underpinning pathways of osteoporosis have not been fully explored yet. Therefore, the screening of OP-associated hub genes as novel therapeutic targets is required.

It is important to note that microarray data analysis can be used to pinpoint crucial genes and gene regulatory networks associated with a disease [11-13]. In this manuscript, we downloaded the OP microarray dataset from the Gene Expression Omnibus (GEO) database and processed it to screen for differentially expressed genes (DEGs) and hub genes across the blood samples of OP patients and normal individuals. Later on, Expression validation on clinical OP samples from the Pakistani population, Gene Ontology (GO) [14], Kyoto Encyclopedia of Genes and Genomes (KEGG) [15] enrichment analyses, and ceRNA network analysis of hub genes were also done in this study. In a nutshell, this study aimed to figure out a few key genes involved in the development and progression of OP, which may be used as potential biomarkers and therapeutic targets for OP patients.

Methods

Sample collection for molecular analyses

The present study included a total of 15 OP subjects (Table S1) who visited the DHQ, Teaching Hospital, Dera Ismail Khan, KPK, Pakistan and voluntarily participated. During the recruitment process, comprehensive information was collected, including details on nutrition, overall health, complete medical history, fracture history, and associated risk factors. To conduct the study, a 5 cc blood sample was obtained from each patient. Additionally, as a control group, 5 cc blood samples were collected from 15 normal individuals. The serum was separated and discarded, and the blood cells were stored at -80 degrees Celsius for further analyses. The study received ethical approval in accordance with the Helsinki Declaration and informed written consent was obtained from all participants.

Data resources

To conduct bioinformatics analysis, we employed an in silico methodology previously described by Wu et al. [16], which involved the following steps: Initially, to identify DEGs and hub genes, the GSE35959 was acquired from the Gene Expression Omnibus (GEO) database (http://www.ncbi.nlm.nih.gov/geo/) [17-19]. This dataset contained the expression profiles of 14 normal individuals and 5 OP patients. Next, two more datasets (GSE56815 and GSE56814) were also retrieved from the GEO database to validate the expression levels of the identified hub genes. Together, these two datasets contained the expression profiles of 64 normal individuals and 67 OP patients. GSE35959, GSE56815, and GSE56814 datasets were based on the GPL20115 platform.

Screening of DEGs

For this purpose, probes in GSE35959, GSE56815, and GSE56814 data files were annotated. Those probes which were not matched with any gene symbol were removed. Moreover, wherever more than one probe was matched to a single gene, the average value of these probes was taken as the final expression value. The FPKM expression values were obtained from GSE35959, GSE56815, and GSE56814 and subjected to differential expression analysis using the limma package in R [20]. For DEGs selection, $|log2FC| > 1$ and p-value < 0.05 were selected as the cutoff criteria.

Protein-protein interaction (PPI) network and hub genes recognition

For PPI network construction, the Search Tool for the Retrieval of Interacting Genes (STRING, https://string-db.org/) [21-23] was conducted

in this study with a minimum score of 0. For hub gene recognition, a Cytohubba plug-in application of the Cytoscape tool [24] was utilized. In this application, the degree method was used to recognize the top eight DEGs as hub genes.

lncRNA-miRNA-mRNA regulatory network

To expand the potential lncRNA-miRNA-mRNA regulatory network associated with the hub genes, we utilized several online databases. Firstly, miRTarBase (http://mirtarbase.mbc.nctu.edu.tw/) [25, 26] and miRDB (http://www.mirdb.org) [27, 28] were employed for miRNA prediction. Next, we used the MiRcode repository (http://www.mircode.org/) [29] to predict lncRNAs targeting miRNAs. Ultimately, we integrated the lncRNA-miRNA-mRNA regulatory network using Cytoscape.

Functional enrichment

Functional enrichment profiling of the hub genes was carried out using the DAVID tool [30]. Functional enrichment includes Gene ontology (GO) and KEGG pathway enrichment. GO is further divided into biological processes (BP), cellular components (CC), and molecular functions (MF) analyses [31]. A $P < 0.05$ was used as the cutoff criterion for the functional enrichment analysis.

Drug prediction analysis

DrugBank (http://www.drugbank.ca) database [32], which contains around seven thousand drug entries and four thousand protein data points was used in this study to evaluate hub genes-associated potential targeted drugs.

Genomic RNA isolation

Total cell RNA from blood cells was extracted using the Trizol method [33]. We employed the NanoDrop 2000 Spectrophotometer (Thermo Fisher Scientific, Waltham, MA, USA) to assess the concentration and purity of the extracted RNA, ensuring that the A260/A280 ratio fell within the range of 1.8 to 2.0.

RT-qPCR validation analysis of hub genes

The specific protocols are as follows: First, the PrimeScript™ RT reagent kit (Takara, Japan) was used for reverse transcription of the extracted RNA from OP patients and control samples into complementary DNA. Then, the RT-qPCR was carried out on an ABI ViiA 7 Real Time PCR System (Thermo Fisher, USA) with a SuperReal SYBR Green Premix Plus (Tiangen Biotech, China) as a fluorescent dye. The GAPDH gene was chosen as the internal reference in the present study. All the experiments were in triplicate independently. The $2^{-\Delta\Delta Ct}$ method was employed to evaluate the relative expression of each hub gene [34]. Student t-test [35] was used to evaluate differences in the expression levels between OP and the normal control group. Primers of each hub gene and control gene (GAPDH), highlighted in **Table 1**, were synthesized from the ORIGENE Company, USA.

ROC curve generation

Based on the RT-qPCR expression data, ROC curves of identified hub gene expression were generated using the SRPLOT web source (https://bioinformatics.com.cn/srplot).

Results

DEGs identification in GSE35959 dataset

In the current study, via GEO2R analysis of the GSE35959 dataset, we identified a total of 2124 DEGs (**Figure 1**) with altered expression levels and 52551 non-DEGs with no alterations in expression levels across 5 blood samples of OP patients relative to 14 normal controls (**Figure 1**). Out of the 2124 DEGs (**Figure 1**), the top 20 significant ($P < 0.05$) DEGs including ten overexpressed and ten down-regulated genes were considered for further analysis (**Table 2**).

PPI network construction and hub gene screening

To gain a deeper knowledge about a few key genes, which are mainly associated with OP, the predefined top 20 DEGs were subjected to STRING analysis. The criterion which was used for STRING analysis includes an interaction score of less than 0.4. A total of 15 DEGs were included in the constructed PPI network, which were linked with one another via 16 edges (**Figure 2**). In this PPI network, the top eight DEGs were declared as hub genes based on the degree and MCC methods using the CytoHubba plugin application of the Cytoscape software (**Figure 2**). The selected eight hub genes were Splicing Factor 3a Subunit 1 (SF3A1),

Table 1. Detail of the primers used for the amplification of hub and control genes

Sr. No	Gene	Gene ID	Primer ID	Product size (bp)
1	GAPDH	2597	GAPDH-F 5'-ACCCACTCCTCCACCTTTGAC-3'	132
			GAPDH-R 5'-CTGTTGCTGTAGCCAAATTCG-3'	
2	SF3A1	10291	SF3A1-F 5'-CCAGACCAAGTCATTGTGCGGA-3'	145
			SF3A1-R 5'-TTGCTGGCAGGAATCTTCTCCC-3'	
3	ATXN2L	11273	ATXN2L-F 5'-CGCAGCAACACCAGGAGA-3'	137
			ATXN2L-R 5'-GCAGCATTCTGGAATTGTTGTA-3'	
4	HSP90B1	7184	HSP90B1-F 5'-GTTTCCCGTGAGACTCTTCAGC-3'	141
			HSP90B1-R 5'-ATTCGTGCCGAACTCCTTCCAG-3'	
5	CD74	972	CD74-F 5'-AAGCCTGTGAGCAAGATGCGCA-3'	154
			CD74-R 5'-AGCAGGTGCATCACATGGTCCT-3'	
6	DHX29	54505	DHX29-F 5'-CCCTCCAGGAGTCAGGAAGA-3'	134
			DHX29-R 5'-ACTGACAAACGTCTCCACCAA-3'	
7	ALG5	29880	ALG5-F 5'-GAGAAGCAGCTTCACGGACGTT-3'	140
			ALG5-R 5'-GTCCAGTTGACAGCAATTTCTGC-3'	
8	NUDCD2	134492	NUDCD2-F 5'-GAGCCGTGTGCCTGCGTG-3'	135
			NUDCD2-R 5'-CAGTCATCCCTCTGACACCGTG-3'	
9	RAB2A	5862	RAB2A-F 5'-AGTTCGGTGCTCGAATGATAAC-3'	128
			RAB2A-R 5'-AATACGACCTTGTGATGGAACG-3'	

Ataxin 2 Like (ATXN2L), Heat Shock Protein 90 Beta Family Member 1 (HSP90B1), Cluster of Differentiation 74 (CD74), DExH-Box Helicase 29 (DHX29), ALG5 Dolichyl-Phosphate Beta-Glucosyltransferase (ALG5), NudC Domain Containing 2 (NUDCD2), and Ras-related protein Rab-2A (RAB2A) (**Figure 2**).

Confirmation of the hub gene expression on additional Gene Expression Omnibus datasets

To confirm the reliability of expression variations among hub genes, we took FPKM values of the hub genes from GSE68815 and GSE68814 datasets to draw the expression box plots of each gene between OP and normal samples (**Figure 3**). After applying the student t-test on the FPKM values, we revealed that SF3A1, ATXN2L, and CD74 were significantly ($P < 0.05$) down-regulated, while HSP90B1, DHX29, ALG5, NUDCD2, and RAB2A were significantly ($P < 0.05$) up-regulated in OP samples relative to the control samples (**Figure 3**).

lncRNA-miRNA-mRNA regulatory network construction of hub genes

Upon analyzing data from various online databases, we observed that a total of 96 miRNAs were found to target all eight hub genes (SF3A1, ATXN2L, HSP90B1, CD74, DHX29, ALG5, NUDCD2, and RAB2A) (**Figure 4A**). By considering the degree of centrality and making intersections, we identified eight potential miRNAs (has-mir-24-3p, has-let-7f-5p, has-mir-155-5p, has-mir-100-5p, has-let-7a-5p, has-mir-1-3p, has-mir-16-5p, and has-let-7b-5p) that collectively target all the hub genes (**Figure 4B**). Further analysis revealed that these 8 miRNAs were targeted by 142 lncRNAs (**Figure 4C**), out of which six lncRNAs (KCNQ1OT1, TMEM-AS, HELLPAR, XIST, NEAT1, and HCG18) were targeting all 6 miRNAs (has-mir-24-3p, has-let-7f-5p, has-mir-16-5p, has-let-7a-5p, has-let-7b-5p, and has-mir-155-5p) (**Figure 4D**).

Gene ontology analysis of hub genes

In this study, we performed a comprehensive GO analysis, which involved using the DAVID tool to predict the BP, CC, and MF associated with the hub genes. **Figure 5A** illustrates the specific biological processes related to hub genes in both OP patients and normal individuals. Furthermore, **Figure 5B** and **5C** highlight the cellular components and molecular function terms associated with the hub genes in the same groups, respectively.

Hub genes exhibited a substantial enrichment in "Sarcoplasmic reticulum lumen, Reg. of mature B cell apoptotic proc, Macrophage

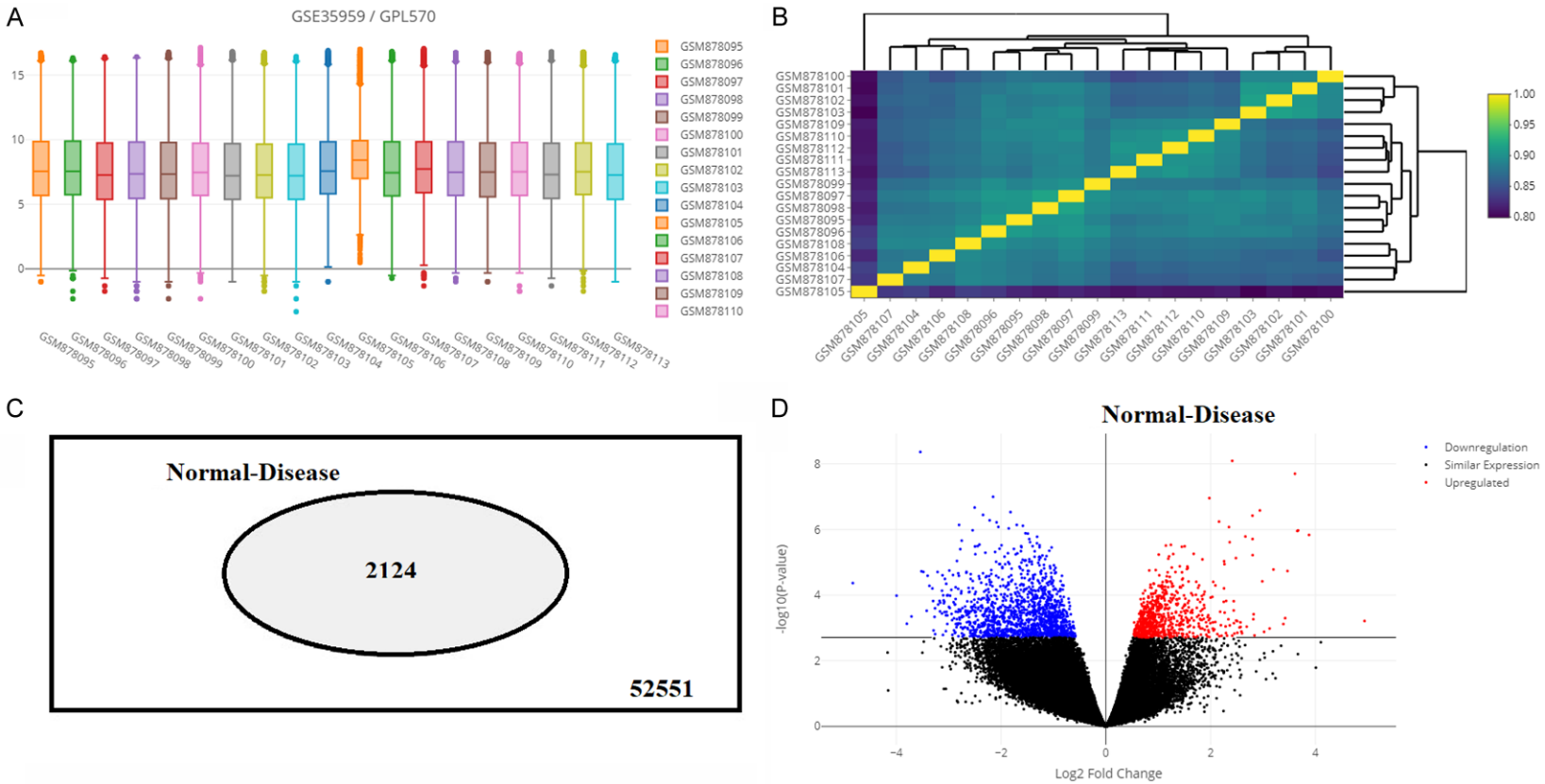

Figure 1. Analyzing gene expression patterns, sample clustering, quantifying differentially expressed genes (DEGs) and non-DEGs, and creating a volcano plot specifically for DEGs within the GSE35959 dataset. (A) Expression-wise comparison of samples in the GSE35959 dataset, (B) Expression-based clustering of samples in the GSE35959 dataset, (C) A total count of DEGs and non DEGs in GSE35959 dataset, and (D) A volcano graph of DEGs in the GSE35959.

Table 2. Top 20 DEGs among OP samples relative to control group in GSE35959

Sr. No	Gene symbol	Expression Status	Log FC	Adjust P
1	CKM	Up-regulation	4.31E-09	4.31E-09
2	DHX29	Up-regulation	2.411926198	8.06E-09
3	HSP90B1	Up-regulation	3.609774064	1.98E-08
4	NUDCD2	Up-regulation	1.975149543	1.10E-07
5	NNMT	Up-regulation	2.939904325	2.62E-07
6	METTL9	Up-regulation	2.799329575	3.78E-07
7	RAB2A	Up-regulation	2.161049449	5.73E-07
8	UBE4B	Up-regulation	2.349702084	8.39E-07
9	WFDC21P	Up-regulation	3.670100767	1.07E-06
10	ALG5	Up-regulation	3.655075383	1.11E-06
11	PPDPF	Down-regulation	2.153952004	1.01E-07
12	CD74	Down-regulation	2.505277038	2.11E-07
13	ADAMTS2	Down-regulation	1.820451671	2.92E-07
14	ATXN2L	Down-regulation	2.087129790	6.22E-07
15	KCTD13	Down-regulation	1.583973054	7.68E-07
16	ZDHHC8	Down-regulation	2.052905155	8.31E-07
17	CBX4	Down-regulation	2.54363072	1.05E-06
18	SF3A1	Down-regulation	1.53564268	1.30E-06
19	UAP1L1	Down-regulation	1.490852211	1.33E-06
20	PLBD2	Down-regulation	1.312445058	1.65E-06

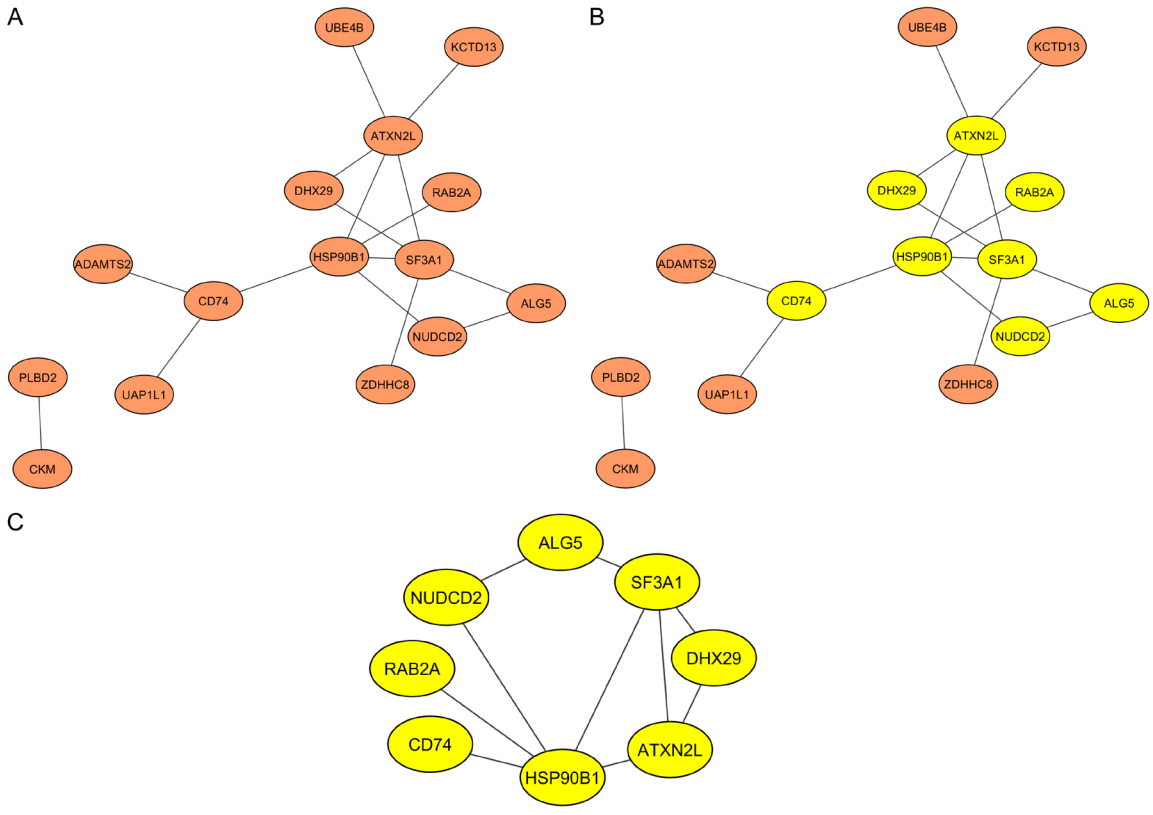

Figure 2. A PPI network of the top 20 DEGs (10 up-regulated and 10 down-regulated) and the selected hub genes. (A) A PPI network of top 20 DEGs, (B) A PPI network of top 20 DEGs highlighting selected hub genes, and (C) A PPI network of the hub genes.

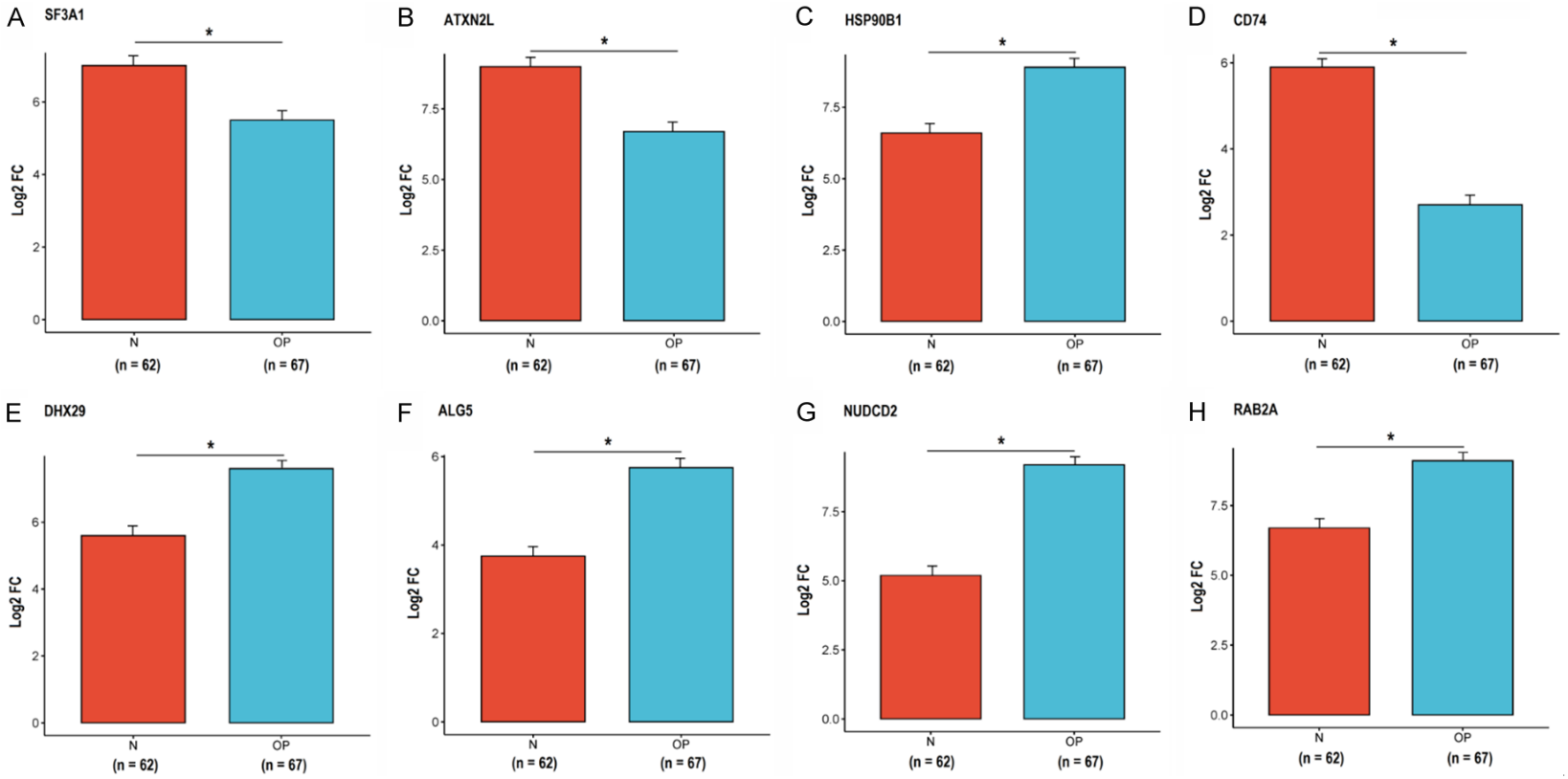

Figure 3. Validation results for the mRNA expression levels of 8 selected hub genes. To validate these genes, we used the GSE56815 and GSE56814 datasets. Each of the selected genes (A) SF3A1, (B) ATXN2L, (C) HNSP90B1, (D) CD74, (E) DHX29, (F) ALG5, (G) NUDCD2, and (H) RAB2A underwent validation. * = *P*-value < 0.05.

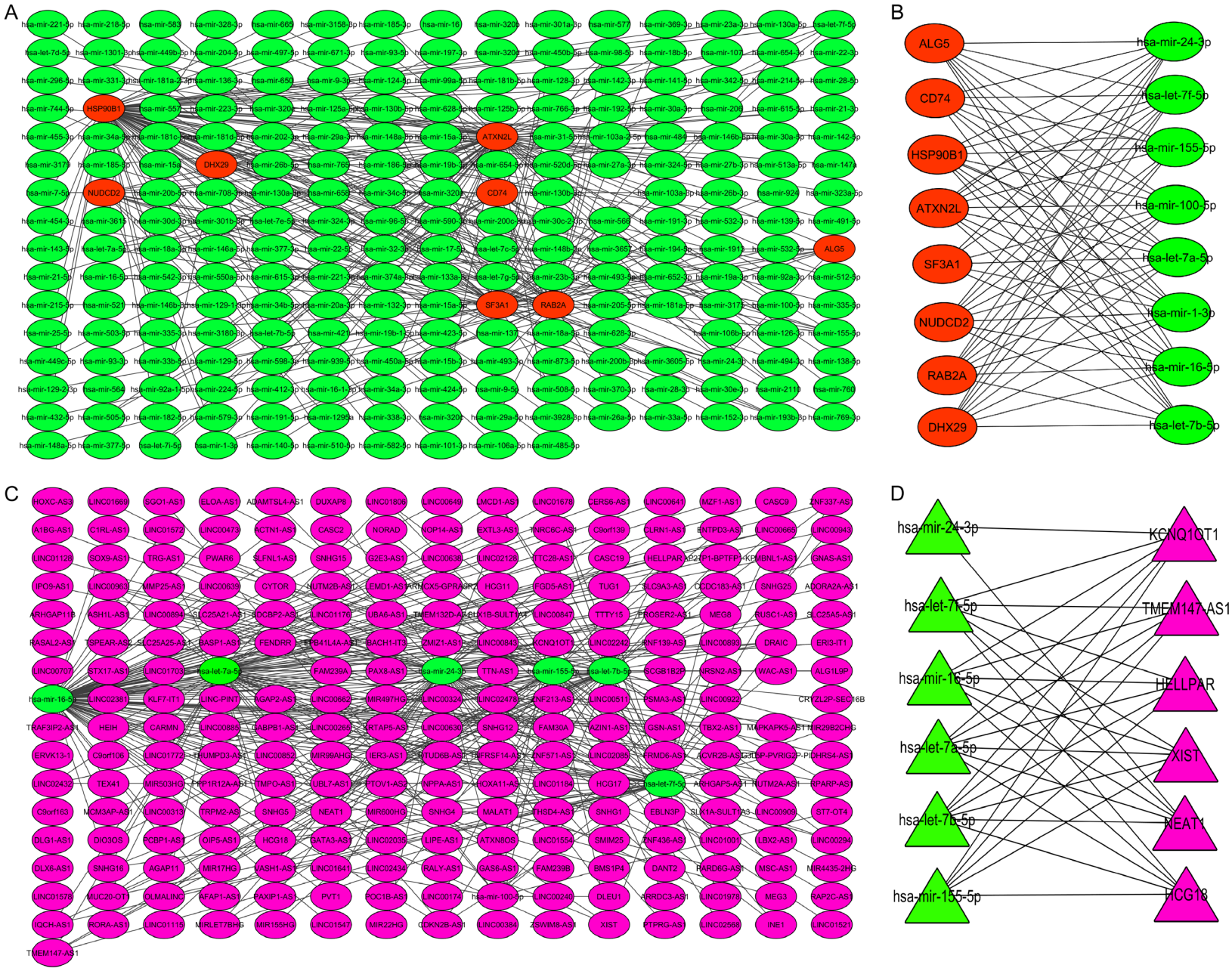
A
B
ALG5
CD74
HSP90B1
ATXN2L
SF3A1
NUDCD2
RAB2A
DHX29
hsa-mir-24-3p
hsa-let-7f-5p
hsa-mir-155-5p
hsa-mir-100-5p
hsa-let-7a-5p
hsa-mir-1-3p
hsa-mir-16-5p
hsa-let-7b-5p
C
D
KCNQ1OT1
TMEM147-AS1
HELLPAR
XIST
NEAT1
HCG18

Figure 4. Networks highlighting associations between miRNAs, lncRNAs, and hub genes. (A) A network of overall predicted miRNAs targeting hub genes, (B) A network between meaningful miRNAs and hub genes, (C) A network of six miRNAs and overall lncRNAs targeting miRNAs, and (D) A network of miRNAs and meaningful lncRNAs. The green nodes are the miRNAs, red nodes are hub genes, while purple nodes are lncRNAs.

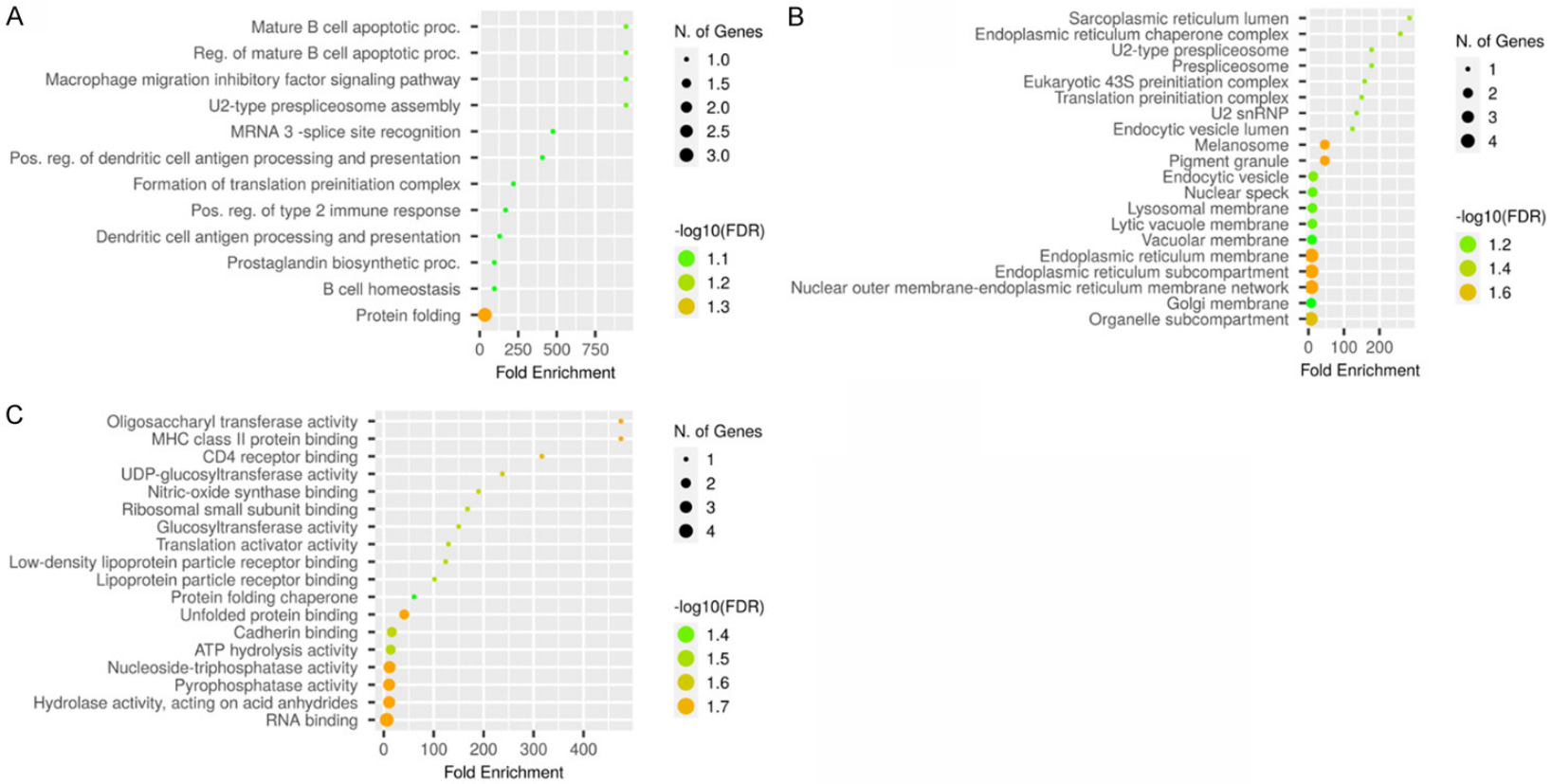

Figure 5. Gene ontology (GO) enrichment analysis of hub genes utilizing the DAVID tool. (A) Biological Process (BP) Terms: This section focuses on the enrichment analysis results related to biological processes associated with the hub genes, (B) Cellular Component (CC) Terms: This section elaborates on the enrichment analysis results concerning the cellular components linked to the hub genes, and (C) Molecular Function (MF) Terms: Here, the legend provides insights into the enrichment analysis findings related to the molecular functions of the hub genes. A $P < 0.05$ was regarded as the selection criteria.

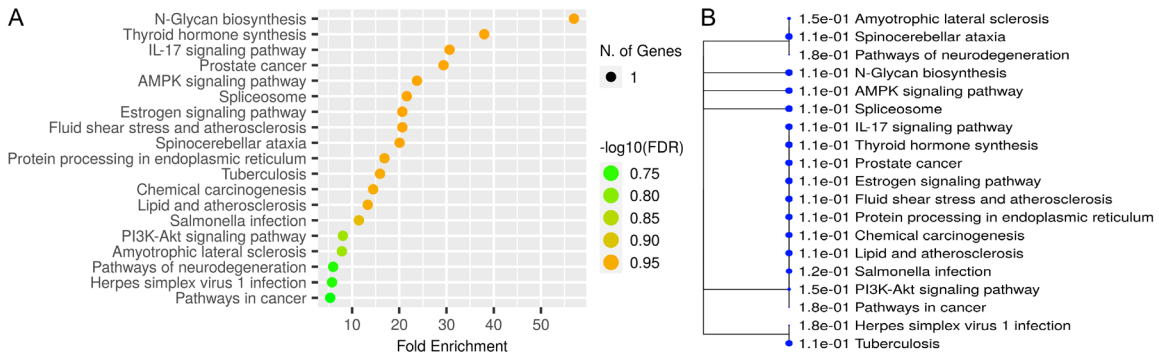

Figure 6. Kyoto encyclopedia of genes and genomes (KEGG) enrichment analysis of hub genes conducted with the DAVID tool. (A) KEGG Terms: This section presents the results of the KEGG enrichment analysis, highlighting the specific KEGG pathways associated with the hub genes, and (B) KEGG Terms Phylogram: Here, the legend describes the representation of the KEGG terms in a phylogenetic tree-like structure. A $P < 0.01$ was regarded as the selection criteria.

migration inhibitory factor signaling pathway, U2-type prespliceosome assembly, and MRNA 3-splice site recognition, etc.", BP terms (**Figure 5A**). Regarding CC, the identified hub genes displayed prominent enrichment in the "Sarcoplasmic reticulum lumen, Endoplasmic reticulum chaperone complex, U2-type prespliceosome, Prespliceosome, Eukarytic 43S preintiation complex, Translation preintiation complex, and U2 snRNP, etc.", CC terms (**Figure 5B**). Concerning MF, the identified hub genes primarily participated in "Oligosaccharyl transferase activity, MHC class II protein binding, CD4 receptor binding, UDP, glucosyltransferase activity, Nitric oxide synthase binding, Ribosomal small subunit binding, Glucosyltrans ferase activity, and Translation activator activity, etc.", MF terms (**Figure 5C**).

Kyoto encyclopedia of genes and genomes analysis of hub genes

In order to gain a deeper insight into the selected hub genes (SF3A1, ATXN2L, HSP90B1, CD74, DHX29, ALG5, NUDCD2, and RAB2A), we also conducted KEGG pathway analysis using the DAVID tool. Hub genes were predominantly concentrated in "N-Glycan biosynthesis, Thyroid hormone synthesis, IL-17 signaling pathway, Prostate cancer, AMPK signaling pathway, Spliceosome, Estrogen signaling pathway, and Fluid shear stress and atherosclerosis, etc.", KEGG terms (**Figure 6**).

Drug prediction analysis of hub genes

For patients afflicted with OP, medical treatment stands as the primary option to address the disease. Hence, it becomes imperative to identify appropriate candidate drugs that hold potential for treatment. In this study, we utilized the DrugBank database to explore suitable therapeutic drugs associated with the identified hub genes, aimed at addressing osteoporosis effectively. For example, Acetaminophen and Cyclosporine drugs were identified as the positive expression regulators of SF3A1 mRNA expression (**Table 3**) while Dronabinol was identified as the negative expression regulator of RAB2A mRNA expression (**Table 3**).

Validation of SF3A1, ATXN2L, HSP90B1, CD74, DHX29, ALG5, NUDCD2, and RAB2A gene expression in clinical OP samples via RT-qPCR

To validate the results obtained from the GEO expression dataset, cDNA from both OP and control blood samples was utilized for RT-qPCR analysis of SF3A1, ATXN2L, HSP90B1, CD74, DHX29, ALG5, NUDCD2, and RAB2A. The results, as depicted in **Figure 7A**, demonstrated that SF3A1, ATXN2L, and CD74 were significantly ($P < 0.05$) down-regulated, while HSP90B1, DHX29, ALG5, NUDCD2, and RAB2A were significantly up-regulated in the OP sample group ($n = 15$) compared to the control group ($n = 15$). Additionally, the ROC curves for SF3A1 (AUC: 1.0, *p*-value < 0.05), ATXN2L (AUC: 1.0, *p*-value < 0.05), HSP90B1 (AUC: 1.0, *p*-value < 0.05), CD74 (AUC: 1.0, *p*-value < 0.05), DHX29 (AUC: 1.0, *p*-value < 0.05), ALG5 (AUC: 1.0, *p*-value < 0.05), NUDCD2 (AUC: 1.0, *p*-value < 0.05), and RAB2A (AUC: 1.0, *p*-value < 0.05) exhibited significant diagnostic potential, sensitivity, and specificity (**Figure 7B**). Notably, the SLC4A4 gene demonstrated the ability to

Table 3. Drug Bank-based hub genes-associated drugs

Sr. No	Hub gene	Drug name	Effect	Reference	Group
1	SF3A1	Acetaminophen	Increase expression of SF3A1 mRNA	A20418	Approved
		Cyclosporine		A21868	
2	ATXN2L	Cyclosporine	Increase expression of ATXN2L mRNA	A21868	Approved
		Silicon dioxide		A20414	
3	HNSP90B1	Isotretinoin	Increase expression of HNSP90B1 mRNA	A24023	Approved
4	CD74	Quercetin	Decrease expression of CD74 mRNA	A23761	Approved
		Cyclosporine		A21868	
5	DHX29	Quercetin	Decrease expression of DHX29 mRNA	A23761	Approved
6	ALG5	Cyclosporine	Decrease expression of ALG5 mRNA	A23761	Approved
7	NUDCD2	Cyclosporine	Decrease expression of NUDCD2 mRNA	A23761	Approved
		Quercetin		A23761	
8	RAB2A	Dronabinol	Decrease expression of RAB2A mRNA	A22519	Approved

distinguish patient tissues from healthy tissues, with a cutoff point ranging from 0.671 to 1.9 (**Figure 7B**).

Discussion

Annually, millions of people around the globe continue to be affected by OP [36]. OP is mainly characterized by impaired bone microarchitecture and the loss of bone mass and strength, especially in elderly individuals. Osteoporotic fractures may be avoided with prompt OP treatment. However, the existing method of treating OP is the least effective because of its time-consuming nature, expensive cost, and other adverse side effects of medicine [37]. Therefore, additional studies exploring bone biology, underpinning molecular pathways, and signaling networks involved in OP will help to understand the nature of this disease which may lead to the discovery of new treatment methods. Moreover, as OP is clinically a silent disease until the fracture occurs, timely diagnosis of this disease is very critical for treating OP and reliving the patient's pain [38]. The current manuscript is based on a variety of Bioinformatics experiments, involving differential expression analysis, PPI network construction, hub genes identification, expression validation, ceRNA network analysis, GO, KEGG, and drug prediction analysis of OP and normal samples across GEO database.

OP patients and normal individual groups in the GSE35959 GEO dataset were subjected to expression analysis to identify DEGs and hub genes between these two groups in the present study. After expression analysis, we identified a total of 2124 DEGs between OP and normal groups with altered expression levels. Out of the 2124 DEGs, the top 20 significant ($P < 0.05$) DEGs including ten overexpressed and ten down-regulated genes, shown in **Table 2**. Moreover, based on expression analysis using the GEO expression dataset and clinical OP samples from the Pakistani population, the eight selected hub genes include significantly ($P < 0.05$) down-regulated SF3A1, ATXN2L, and CD74, while significantly ($P < 0.05$) up-regulated HSP90B1, DHX29, ALG5, NUDCD2, and RAB2A in OP samples relative to the controls.

SF3A1 encodes for a subunit of the splicing factor 3a protein complex, which plays a critical role in the assembly of the spliceosome and mRNA splicing event [39]. According to earlier studies, the down-regulation of the SF3A1 gene is associated with Paget's disease of bone (PDB) [40]. The protein encoded by the ATXN2L gene belongs to the spinocerebellar ataxia (SCAs) family, which is mainly associated with neurodegenerative disorders [41, 42]. To the best of our knowledge, the role of this gene has not been explored in OP so far, we are the first to report the down-regulation of this gene in OP patients. The CD74 coding protein serves as a receptor for the cytokine macrophage migration inhibitory factor [43]. Mice deficient in the CD74 protein exhibited increased osteoclastogenesis and bone mass loss [44]. The HSP90B1 coding protein plays an important role in protein folding during the secretory pathway [45, 46]. The abnormal expression of HSP90B1 was also found to be associated with PDB disease [47]. The protein produced by DHX29 is a key player in the innate immune response among

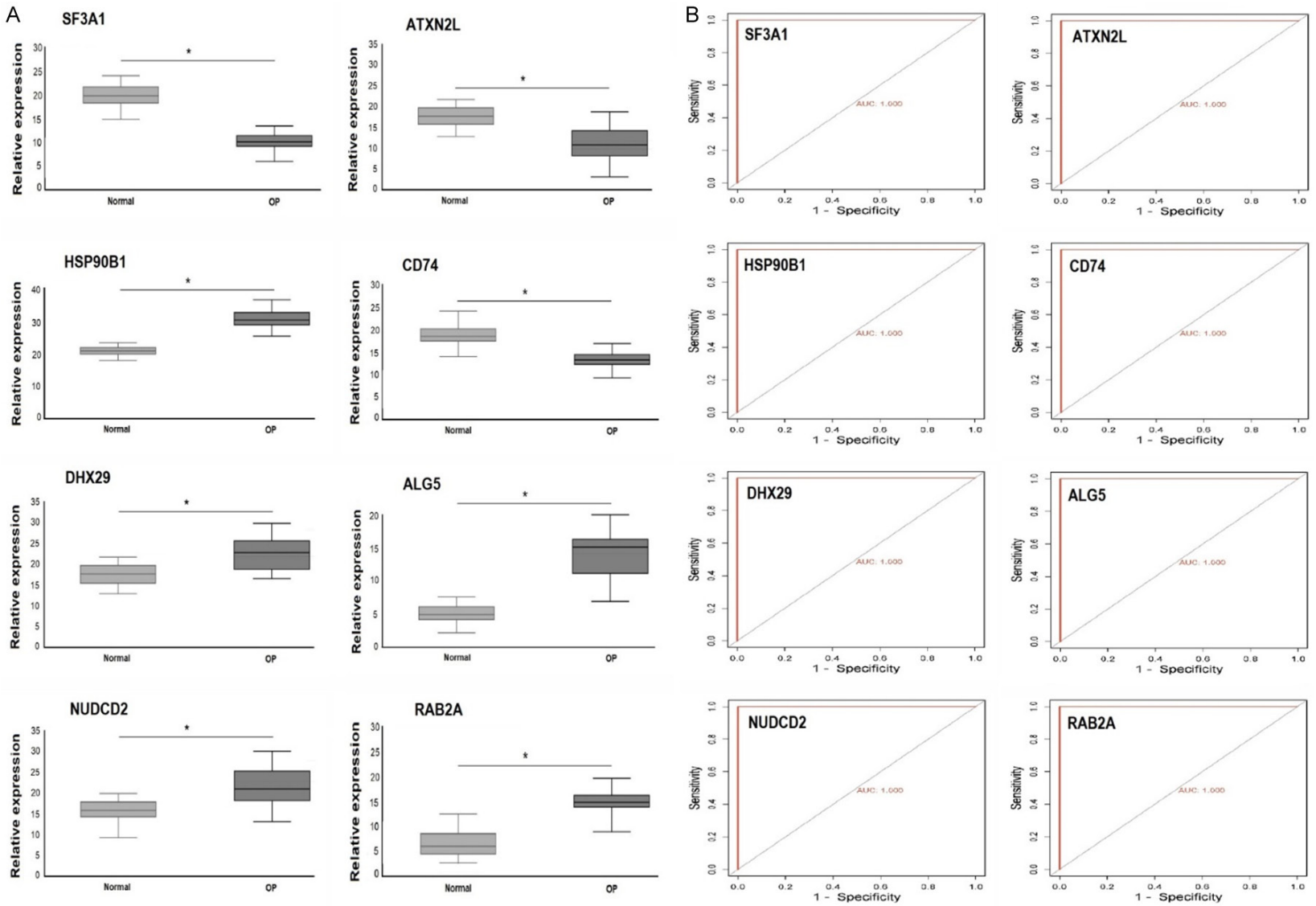

Figure 7. Relative expression and ROC curve analysis of the hub genes in Pakistani OP patients and normal controls. (A) Relative expression analysis of the hub genes in Pakistani OP patients and control samples via RT-qPCR, and (B) RT-qPCR expression-based ROC curves of the identified hub genes. * = *P*-value < 0.05.

humans [48]. The overexpression of DHX29 is associated with the bone metastasis of a variety of cancers including lung cancer [49, 50]. The ALG5 coding protein is an important enzyme required for the addition of glucose molecules to N-glycan precursors [51]. The dysregulation of ALG5 is associated with bone disease [52]. The protein encoded by NUDCD2 plays an important role in cell cycle progression and cell migration [53]. To the best of our knowledge, the role of this gene has not been explored in OP so far, we are the first to report its down-regulation in OP patients. The RAB2A coding protein is responsible for intracellular membrane trafficking of the proteins [54]. The up-regulation of RAB2A is associated with the development of OP [55, 56].

Currently, various studies have shown that lncRNAs, circRNAs, and miRNAs are the important causative factors of many diseases such as neurodegenerative diseases by interacting with disease-causing mRNAs [57]. For example, *Dandan et al.* revealed that circRNA-vgll3 leads to enhanced osteogenic differentiation of adipose-derived mesenchymal stem cells in OP patients [58]. Similarly, *Xiqiang et al.* highlighted that circRNA-0011269 can cause osteoporosis development and progression by dysregulating the RUNX2 gene in combination with miR-1229. The proper relationship between lncRNAs, miRNAs, and mRNAs in OP is still dim. Therefore, in this study, we constructed the lncRNA-miRNA-mRNA regulatory network of the hub genes (**Figure 5**), which will help to gain new insight into the disease physiology of OP [59].

In the present study, we have also identified hub genes which are associated with important molecular pathways including N-Glycan biosynthesis [60], Thyroid hormone synthesis [61], IL-17 signaling pathway [62], Prostate cancer [63], AMPK signaling pathway [64], Spliceosome [65], Estrogen signaling pathway [66], and Fluid shear stress and atherosclerosis [67]. The roles of these pathways are already established in the development of OP. Lastly, a few hub gene expression regulatory drugs were also predicted in this study, which is already in clinical use, suggesting that the identified hub genes are closely associated with the development of OP. The current study has a few important limitations that should be considered. Firstly, this study is purely based on the bioinformatics analysis and expression datasets, as well as the expression of predicted miRNAs, and lncRNAs remain unchecked, which is a common situation in predicting ceRNA networks. Secondly, the underlying mechanisms of the ceRNA network have not been validated through molecular experiments; therefore, additional research work based on molecular experiments is needed to be done for the validation of our conclusion.

Conclusion

Through the integration of a comprehensive bioinformatics analysis and molecular experimental approach, we have successfully identified and validated a set of crucial hub genes (SF3A1, ATXN2L, HSP90B1, CD74, DHX29, ALG5, NUDCD2, and RAB2A) in patients with OP. These hub genes hold significant potential as critical regulators and biomarkers for OP, playing a vital role in the pathogenesis and progression of the disease.

Acknowledgements

The authors extend their appreciation to Taif University, Saudi Arabia, for supporting this work through project number (TU-DSPP-2024-15).

Disclosure of conflict of interest

None.

Address correspondence to: Guang Chen, Department of Orthopedic Surgery, The Second Hospital of Dalian Medical University, Dalian, Liaoning, China. E-mail: chenguang987123@126.com; Yasir Hameed, Department of Biotechnology, Institute of Biochemistry Biotechnology, and Bioinformatics, The Islamia University of Bahawalpur, Pakistan. E-mail: yasirhameed2011@gmail.com; Rida Naz, Regional Blood Centre, KPK Health Program, Dera Ismail Khan 29050, Pakistan. E-mail: dr.ridaanaz@gmail.com

References

[1] Li H, Li T, Fan J, Li T, Fan L, Wang S, Weng X, Han Q and Zhao RC. miR-216a rescues dexamethasone suppression of osteogenesis, promotes osteoblast differentiation and enhances bone formation, by regulating c-Cbl-mediated PI3K/AKT pathway. Cell Death Differ 2015; 22: 1935-1945.

[2] Compston J, Cooper A, Cooper C, Gittoes N, Gregson C, Harvey N, Hope S, Kanis JA, McCloskey EV, Poole KES, Reid DM, Selby P, Thompson F, Thurston A and Vine N; National Osteoporosis Guideline Group (NOGG). UK clinical guideline for the prevention and treatment of osteoporosis. Arch Osteoporos 2017; 12: 43.
[3] Tarantino U, Iolascon G, Cianferotti L, Masi L, Marcucci G, Giusti F, Marini F, Parri S, Feola M, Rao C, Piccirilli E, Zanetti EB, Cittadini N, Alvaro R, Moretti A, Calafiore D, Toro G, Gimigliano F, Resmini G and Brandi ML. Clinical guidelines for the prevention and treatment of osteoporosis: summary statements and recommendations from the Italian Society for Orthopaedics and Traumatology. J Orthop Traumatol 2017; 18 Suppl 1: 3-36.
[4] Tanaka KI, Xue Y, Nguyen-Yamamoto L, Morris JA, Kanazawa I, Sugimoto T, Wing SS, Richards JB and Goltzman D. FAM210A is a novel determinant of bone and muscle structure and strength. Proc Natl Acad Sci U S A 2018; 115: E3759-E3768.
[5] Uehara S, Udagawa N, Mukai H, Ishihara A, Maeda K, Yamashita T, Murakami K, Nishita M, Nakamura T, Kato S, Minami Y, Takahashi N and Kobayashi Y. Protein kinase N3 promotes bone resorption by osteoclasts in response to Wnt5a-Ror2 signaling. Sci Signal 2017; 10: eaan0023.
[6] Yang X, Zhu S, Li L, Zhang L, Xian S, Wang Y and Cheng Y. Identification of differentially expressed genes and signaling pathways in ovarian cancer by integrated bioinformatics analysis. Onco Targets Ther 2018; 11: 1457-1474.
[7] Boyce BF, Li J, Xing L and Yao Z. Bone remodeling and the role of TRAF3 in osteoclastic bone resorption. Front Immunol 2018; 9: 2263.
[8] Xia B, Li Y, Zhou J, Tian B and Feng L. Identification of potential pathogenic genes associated with osteoporosis. Bone Joint Res 2017; 6: 640-648.
[9] Foj L and Filella X. Identification of potential miRNAs biomarkers for high-grade prostate cancer by integrated bioinformatics analysis. Pathol Oncol Res 2019; 25: 1445-1456.
[10] Xie HX, Cao L, Ye LL, Shan G, Jiang C and Song W. Identification of candidate genes for osteoporosis via integrated bioinformatics analysis. Indian J Pharm Sci 2021; 6: 6-13.
[11] Ma M, Luo S, Zhou W, Lu L, Cai J, Yuan F and Yin F. Bioinformatics analysis of gene expression profiles in B cells of postmenopausal osteoporosis patients. Taiwan J Obstet Gynecol 2017; 56: 165-170.
[12] Al-Azzawy M. Immunological aspects of ELISA positive PCR negative newly diagnosed hepatitis C patients in Kirkuk province. Al-Kitab J Pure Sci 2020; 3: 154-162.
[13] Ismaeel PA. Out-lab therapy approach based on elected a restriction enzyme to transfer target gene. Al-Kitab J Pure Sci 2019; 2: 197-209.
[14] Cao Y, Li R, Li Y, Zhang T, Wu N, Zhang J and Guo Z. Identification of transcription factor-gene regulatory network in acute myocardial infarction. Heart Lung Circ 2017; 26: 343-353.
[15] Zhang Y, Wang N, Ma J, Chen XC, Li Z and Zhao W. Expression profile analysis of new candidate genes for the therapy of primary osteoporosis. Eur Rev Med Pharmacol Sci 2016; 20: 433-440.
[16] Wu S, Ud Din I, Sadiq FM, Abdel-Maksoud MA, Haris M, Mubarak A, Farrag MA, Alghamdi S, Almekhlafi S, Akram M and Li G. Dysfunctional network of hub genes in hypertrophic cardiomyopathy patients. Am J Transl Res 2022; 14: 8918-8933.
[17] Clough E and Barrett T. The gene expression omnibus database. Methods Mol Biol 2016; 1418: 93-110.
[18] Sial N, Rehman JU, Saeed S, Ahmad M, Hameed Y, Atif M, Rehman A, Asif R, Ahmed H, Hussain MS, Khan MR, Ambreen A and Ambreen A. Integrative analysis reveals methylenetetrahydrofolate dehydrogenase 1-like as an independent shared diagnostic and prognostic biomarker in five different human cancers. Biosci Rep 2022; 42: BSR20211783.
[19] Hameed Y, Usman M, Liang S and Ejaz S. Novel diagnostic and prognostic biomarkers of colorectal cancer: capable to overcome the heterogeneity-specific barrier and valid for global applications. PLoS One 2021; 16: e0256020.
[20] Ritchie ME, Phipson B, Wu D, Hu Y, Law CW, Shi W and Smyth GK. limma powers differential expression analyses for RNA-sequencing and microarray studies. Nucleic Acids Res 2015; 43: e47.
[21] Szklarczyk D, Gable AL, Lyon D, Junge A, Wyder S, Huerta-Cepas J, Simonovic M, Doncheva NT, Morris JH, Bork P, Jensen LJ and Mering CV. STRING v11: protein-protein association networks with increased coverage, supporting functional discovery in genome-wide experimental datasets. Nucleic Acids Res 2019; 47: D607-D613.
[22] Zhang L, Sahar AM, Li C, Chaudhary A, Yousaf I, Saeedah MA, Mubarak A, Haris M, Nawaz M, Reem MA, Ramadan FA, Mostafa AAM, Feng W and Hameed Y. A detailed multi-omics analysis of GNB2 gene in human cancers. Braz J Biol 2022; 84: e260169.
[23] Yasir M, Nawaz A, Ghazanfar S, Okla MK, Chaudhary A, Al WH, Ajmal MN, AbdElgawad H, Ahmad Z, Abbas F, Wadood A, Manzoor Z, Akhtar N, Din M, Hameed Y and Imran M. Antibacterial activity of essential oils against multi-

drug-resistant foodborne pathogens isolated from raw milk. Braz J Biol 2022; 84: e259449.
[24] Shannon P, Markiel A, Ozier O, Baliga NS, Wang JT, Ramage D, Amin N, Schwikowski B and Ideker T. Cytoscape: a software environment for integrated models of biomolecular interaction networks. Genome Res 2003; 13: 2498-2504.
[25] Huang HY, Lin YC, Li J, Huang KY, Shrestha S, Hong HC, Tang Y, Chen YG, Jin CN, Yu Y, Xu JT, Li YM, Cai XX, Zhou ZY, Chen XH, Pei YY, Hu L, Su JJ, Cui SD, Wang F, Xie YY, Ding SY, Luo MF, Chou CH, Chang NW, Chen KW, Cheng YH, Wan XH, Hsu WL, Lee TY, Wei FX and Huang HD. miRTarBase 2020: updates to the experimentally validated microRNA-target interaction database. Nucleic Acids Res 2020; 48: D148-D154.
[26] Khan M and Hameed Y. Discovery of novel six genes-based cervical cancer-associated biomarkers that are capable to break the heterogeneity barrier and applicable at the global level. J Cancer Res Ther 2023; 2023: 9000.
[27] Wang X. miRDB: a microRNA target prediction and functional annotation database with a wiki interface. RNA 2008; 14: 1012-1017.
[28] Usman M and Hameed Y. GNB1, a novel diagnostic and prognostic potential biomarker of head and neck and liver hepatocellular carcinoma. J Cancer Res Ther 2023; 2023: 9000.
[29] Jeggari A, Marks DS and Larsson E. miRcode: a map of putative microRNA target sites in the long non-coding transcriptome. Bioinformatics 2012; 28: 2062-2063.
[30] Huang DW, Sherman BT, Tan Q, Collins JR, Alvord WG, Roayaei J, Stephens R, Baseler MW, Lane HC and Lempicki RA. The DAVID gene functional classification tool: a novel biological module-centric algorithm to functionally analyze large gene lists. Genome Biol 2007; 8: R183.
[31] Harris MA, Clark J, Ireland A, Lomax J, Ashburner M, Foulger R, Eilbeck K, Lewis S, Marshall B, Mungall C, Richter J, Rubin GM, Blake JA, Bult C, Dolan M, Drabkin H, Eppig JT, Hill DP, Ni L, Ringwald M, Balakrishnan R, Cherry JM, Christie KR, Costanzo MC, Dwight SS, Engel S, Fisk DG, Hirschman JE, Hong EL, Nash RS, Sethuraman A, Theesfeld CL, Botstein D, Dolinski K, Feierbach B, Berardini T, Mundodi S, Rhee SY, Apweiler R, Barrell D, Camon E, Dimmer E, Lee V, Chisholm R, Gaudet P, Kibbe W, Kishore R, Schwarz EM, Sternberg P, Gwinn M, Hannick L, Wortman J, Berriman M, Wood V, de la Cruz N, Tonellato P, Jaiswal P, Seigfried T and White R; Gene Ontology Consortium. The gene ontology (GO) database and informatics resource. Nucleic Acids Res 2004; 32: D258-261.
[32] Wishart DS, Knox C, Guo AC, Cheng D, Shrivastava S, Tzur D, Gautam B and Hassanali M. DrugBank: a knowledgebase for drugs, drug actions and drug targets. Nucleic Acids Res 2008; 36: D901-906.
[33] Rio DC, Ares M Jr, Hannon GJ and Nilsen TW. Purification of RNA using TRIzol (TRI reagent). Cold Spring Harb Protoc 2010; 2010: pdb.prot5439.
[34] Livak KJ and Schmittgen TD. Analysis of relative gene expression data using real-time quantitative PCR and the 2(-Delta Delta C(T)) Method. Methods 2001; 25: 402-408.
[35] Mishra P, Singh U, Pandey CM, Mishra P and Pandey G. Application of student's t-test, analysis of variance, and covariance. Ann Card Anaesth 2019; 22: 407-411.
[36] Elonheimo H, Lange R, Tolonen H and Kolossa-Gehring M. Environmental substances associated with osteoporosis-a scoping review. Int J Environ Res Public Health 2021; 18: 738.
[37] Bover J, Bailone L, López-Báez V, Benito S, Ciceri P, Galassi A and Cozzolino M. Osteoporosis, bone mineral density and CKD-MBD: treatment considerations. J Nephrol 2017; 30: 677-687.
[38] Ballas SK, Kesen MR, Goldberg MF, Lutty GA, Dampier C, Osunkwo I, Wang WC, Hoppe C, Hagar W, Darbari DS and Malik P. Beyond the definitions of the phenotypic complications of sickle cell disease: an update on management. ScientificWorldJournal 2012; 2012: 949535.
[39] Nameki N, Takizawa M, Suzuki T, Tani S, Kobayashi N, Sakamoto T, Muto Y and Kuwasako K. Structural basis for the interaction between the first SURP domain of the SF3A1 subunit in U2 snRNP and the human splicing factor SF1. Protein Sci 2022; 31: e4437.
[40] McNeill RE, Miller N and Kerin MJ. Evaluation and validation of candidate endogenous control genes for real-time quantitative PCR studies of breast cancer. BMC Mol Biol 2007; 8: 107.
[41] Kaehler C, Isensee J, Nonhoff U, Terrey M, Hucho T, Lehrach H and Krobitsch S. Ataxin-2-like is a regulator of stress granules and processing bodies. PLoS One 2012; 7: e50134.
[42] Xu W, Li H, Hameed Y, Abdel-Maksoud MA, Almutairi SM, Mubarak A, Aufy M, Alturaiki W, Alshalani AJ, Mahmoud AM and Li C. Elucidating the clinical and immunological value of m6A regulator-mediated methylation modification patterns in adrenocortical carcinoma. Oncol Res 2023; 31: 819-831.
[43] Cho Y, Jones BF, Vermeire JJ, Leng L, DiFedele L, Harrison LM, Xiong H, Kwong YK, Chen Y, Bucala R, Lolis E and Cappello M. Structural and

functional characterization of a secreted hookworm macrophage migration inhibitory factor (MIF) that interacts with the human MIF receptor CD74. J Biol Chem 2007; 282: 23447-23456.
[44] Mun SH, Won HY, Hernandez P, Aguila HL and Lee SK. Deletion of CD74, a putative MIF receptor, in mice enhances osteoclastogenesis and decreases bone mass. J Bone Miner Res 2013; 28: 948-959.
[45] Sriburi R, Bommiasamy H, Buldak GL, Robbins GR, Frank M, Jackowski S and Brewer JW. Coordinate regulation of phospholipid biosynthesis and secretory pathway gene expression in XBP-1(S)-induced endoplasmic reticulum biogenesis. J Biol Chem 2007; 282: 7024-7034.
[46] Usman M, Hameed Y and Ahmad M. Does human papillomavirus cause human colorectal cancer? Applying Bradford Hill criteria postulates. Ecancermedicalscience 2020; 14: 1107.
[47] Vidal RL, Sepulveda D, Troncoso-Escudero P, Garcia-Huerta P, Gonzalez C, Plate L, Jerez C, Canovas J, Rivera CA, Castillo V, Cisternas M, Leal S, Martinez A, Grandjean J, Sonia D, Lashuel HA, Martin AJM, Latapiat V, Matus S, Sardi SP, Wiseman RL and Hetz C. Enforced dimerization between XBP1s and ATF6f enhances the protective effects of the UPR in models of neurodegeneration. Mol Ther 2021; 29: 1862-1882.
[48] Carty M, Guy C and Bowie AG. Detection of viral infections by innate immunity. Biochem Pharmacol 2021; 183: 114316.
[49] Attar-Schneider O, Drucker L and Gottfried M. Migration and epithelial-to-mesenchymal transition of lung cancer can be targeted via translation initiation factors eIF4E and eIF4GI. Lab Invest 2016; 96: 1004-1015.
[50] Khalil T, Okla MK, Al-Qahtani WH, Ali F, Zahra M, Shakeela Q, Ahmed S, Akhtar N, AbdElgawad H, Asif R, Hameed Y, Adetunji CO, Farid A and Ghazanfar S. Tracing probiotic producing bacterial species from gut of buffalo (Bubalus bubalis), South-East-Asia. Braz J Biol 2022; 84: e259094.
[51] Zhang Y, Kong D, Reichl L, Vogt N, Wolf F and Großhans J. The glucosyltransferase Xiantuan of the endoplasmic reticulum specifically affects E-Cadherin expression and is required for gastrulation movements in Drosophila. Dev Biol 2014; 390: 208-220.
[52] Hasan LK, Aljabban J, Rohr M, Mukhtar M, Adapa N, Salim R, Aljabban N, Syed S, Syed S, Panahiazar M, Hadley D and Jarjour W. Meta-analysis reveals genetic correlates of osteoporosis pathogenesis. J Rheumatol 2021; 48: 940-945.
[53] Liu M, Zhang W, Li M, Feng J, Kuang W, Chen X, Yang F, Sun Q, Xu Z, Hua J, Yang C, Liu W, Shu Q, Yang Y, Zhou T and Xie S. NudCL2 is an autophagy receptor that mediates selective autophagic degradation of CP110 at mother centrioles to promote ciliogenesis. Cell Res 2021; 31: 1199-1211.
[54] Stenmark H and Olkkonen VM. The rab gtpase family. Genome Biol 2001; 2: REVIEWS3007.
[55] Yuan W, Yang M and Zhu Y. Development and validation of a gene signature predicting the risk of postmenopausal osteoporosis. Bone Joint Res 2022; 11: 548-560.
[56] Ullah L, Hameed Y, Ejaz S, Raashid A, Iqbal J, Ullah I and Ejaz SA. Detection of novel infiltrating ductal carcinoma-associated BReast CAncer gene 2 mutations which alter the deoxyribonucleic acid-binding ability of BReast CAncer gene 2 protein. J Cancer Res Ther 2020; 16: 1402-1407.
[57] D'Ambra E, Capauto D and Morlando M. Exploring the regulatory role of circular RNAs in neurodegenerative disorders. Int J Mol Sci 2019; 20: 5477.
[58] Zhang D, Ni N, Wang Y, Tang Z, Gao H, Ju Y, Sun N, He X, Gu P and Fan X. CircRNA-vgll3 promotes osteogenic differentiation of adipose-derived mesenchymal stem cells via modulating miRNA-dependent integrin α5 expression. Cell Death Differ 2021; 28: 283-302.
[59] Xu X, Chen Y, Tan B, Wang D, Yuan Z and Wang F. Circular RNA circ_0011269 sponges miR-122 to regulate RUNX2 expression and promotes osteoporosis progression. J Cell Biochem 2020; 121: 4819-4826.
[60] Wang N, Ma S and Fu L. Gut microbiota dysbiosis as one cause of osteoporosis by impairing intestinal barrier function. Calcif Tissue Int 2022; 110: 225-235.
[61] Delitala AP, Scuteri A and Doria C. Thyroid hormone diseases and osteoporosis. J Clin Med 2020; 9: 1034.
[62] Zhao R. Immune regulation of bone loss by Th17 cells in oestrogen-deficient osteoporosis. Eur J Clin Invest 2013; 43: 1195-1202.
[63] Daniell HW. Osteoporosis after orchiectomy for prostate cancer. J Urol 1997; 157: 439-444.
[64] Zhou R, Wang Z and Ma C. Hispidulin exerts anti-osteoporotic activity in ovariectomized mice via activating AMPK signaling pathway. Cell Biochem Biophys 2014; 69: 311-317.
[65] Yan S, Zhang Y, Lu D, Dong F and Lian Y. ECM-receptor interaction as a prognostic indicator for clinical outcome of primary osteoporosis. Int J Clin Exp Med 2016; 9: 9-20.
[66] Raisz LG. Pathogenesis of osteoporosis: concepts, conflicts, and prospects. J Clin Invest 2005; 115: 3318-3325.
[67] Bakker AD, Klein-Nulend J, Tanck E, Heyligers IC, Albers GH, Lips P and Burger EH. Different responsiveness to mechanical stress of bone cells from osteoporotic versus osteoarthritic donors. Osteoporos Int 2006; 17: 827-833.

Table S1. Clinical characteristics of the OP patients

Sr. No	Gender	Age (Years)	Case	BMI
1	Female	47	Advance	24.2
2	Female	55	Advance	23.5
3	Female	51	Advance	23.6
4	Female	45	Advance	22.5
5	Female	53	Advance	24.5
6	Female	52	Advance	24.2
7	Female	62	Advance	29.1
8	Female	54	Advance	19.9
9	Female	49	Advance	21.2
10	Female	56	Advance	22.1
11	Female	61	Advance	22.2
12	Female	45	Advance	26.2
13	Female	55	Advance	23.5
14	Female	56	Advance	22.9
15	Female	46	Advance	20.5

BMI = Body Mass Index.